Carbohydrate Polymers 117 (2015) 43–53

Contents lists available at ScienceDirect

Carbohydrate Polymers

journal homepage: www.elsevier.com/locate/carbpol

A biocompatible calcium salt of hyaluronic acid grafted with polyacrylic acid

Yoshiyuki Nakagawa [a], Satoshi Nakasako [b], Seiichi Ohta [b], Taichi Ito [a,b,*]

[a] Department of Chemical System Engineering, The University of Tokyo, 7-3-1 Hongo, Bunkyo-ku, Tokyo 113-8656, Japan
[b] Center for Disease Biology and Integrative Medicine, The University of Tokyo, 7-3-1 Hongo, Bunkyo-ku, Tokyo 113-0033, Japan

ARTICLE INFO

Article history:
Received 30 November 2013
Received in revised form 23 August 2014
Accepted 8 September 2014
Available online 23 September 2014

Keywords:
Hyaluronic acid
Polyacrylic acid
Controlled radical polymerization
Intraperitoneal administration
Drug delivery
Adhesion-preventing material

ABSTRACT

We have synthesized hyaluronic acid (HA) grafted with polyacrylic acid (PAA) *via* controlled radical polymerization (CRP) in aqueous media. The grafted HA (HA-*g*-PAA) showed slow degradation by hyaluronidase compared with unmodified HA as a result of the steric hindrance produced by grafted PAA, and PAA was detached by hydrolysis and enzymatic degradation by lipase. It formed an insoluble salt immediately after mixing with Ca^{2+} by the binding between grafted PAA and Ca^{2+}. Both HA-*g*-PAA and its salt showed good biocompatibility, especially to mesothelial cells *in vitro*. Finally, they were administered into mice subcutaneously and intraperitoneally. The residue of the material was observed 7 days after subcutaneous administration, while the material was almost cleared from the peritoneum 7 days after intraperitoneal administration with or without Ca^{2+}. HA-*g*-PAA is expected to be applicable to medical uses such as drug delivery in the peritoneum and for materials preventing peritoneal adhesion.

1. Introduction

Hyaluronic acid (HA) is a natural linear polysaccharide of alternating D-glucuronic acid and *N*-acetyl-D-glucosamine found throughout the body (Laurent & Fraser, 1992). HA is widely used for medical applications, such as postsurgical adhesion prevention (Ito et al., 2007b; Yeo et al., 2006b), viscosupplementation (Strauss, Hart, Miller, Altman, & Rosen, 2009), eye drops for dry eyes (Yokoi, Komuro, Nishida, & Kinoshita, 1997), and endoscopic submucosal dissection (Tanaka et al., 2007) because HA can be safely administered to the human body as a result of its nonimmunogenicity (Delmage, Powars, Jaynes, & Allerton, 1986). However, native HA has a short turnover rate and poor mechanical stability (Harada & Takahashi, 2007). Thus, HA has been chemically modified with various approaches, and *in situ* cross-linkable hydrogels composed of HA have been reported utilizing various chemical reactions such as the formation of a Schiff base (Su, Chen, & Lin, 2010), a disulfide bond (Shu, Liu, Luo, Roberts, & Prestwich, 2002), Click reaction (Takahashi et al., 2013), or Michael addition (Jin et al., 2010). Although these modifications achieved local administration of HA-based hydrogels, nonspecific chemical reactions between tissues and reactive functional groups such as aldehyde or thiol groups are unavoidable.

Grafting of a different polymer is an efficient approach to functionalize native polysaccharides. Two approaches, "grafting to" by conjugation and "grafting from" by graft polymerization, are well known (Roy, Semsarilar, Guthrie, & Perrier, 2009). For instance, thermosensitive HA was prepared by the grafting of poly(*N*-isopropylacrylamide) by both approaches (Mazumder, Fitzpatrick, Muirhead, & Sheardown, 2012; Tan et al., 2009). Polyacrylic acid (PAA) or sodium polyacrylate, which is the sodium salt of PAA, can also be a grafting polymer. Many kinds of polysaccharides, such as cellulose derivatives (Mishra, Rani, & Sen, 2012; Ostmark, Harrisson, Wooley, & Malmstrom, 2007), dextran (Thermes et al., 1992), carrageenan (Pourjavadi, Harzandi, & Hosseinzadeh, 2004), chitosan (Chen, Liu, & Tan, 2010), and starch (Pal & Pal, 2012), have been grafted by PAA. However, HA grafted with PAA (HA-*g*-PAA) has not been reported to the best of our knowledge.

Controlled radical polymerization (CRP), including atom transfer radical polymerization (ATRP) (Matyjaszewski & Xia, 2001), is an efficient and convenient method for controlling the molecular weight and distribution of grafted polymers. Recently, acidic monomers such as acrylic acid (Coullerez, Carlmark, Malmstrom, & Jonsson, 2004) and methacrylic acid (Ashford, Naldi, O'Dell,

* Corresponding author at: Center for Disease Biology and Integrative Medicine, The University of Tokyo, 7-3-1 Hongo, Bunkyo-ku, Tokyo 113-0033, Japan. Tel.: +81 3 5841 1698; fax: +81 3 5841 1697.
E-mail addresses: y_nakaga@chemsys.t.u-tokyo.ac.jp (Y. Nakagawa), satoshinakasako@gmail.com (S. Nakasako), s-ohta@chemsys.t.u-tokyo.ac.jp (S. Ohta), taichi@m.u-tokyo.ac.jp, taichi091773ito@yahoo.co.jp (T. Ito).

http://dx.doi.org/10.1016/j.carbpol.2014.09.037
0144-8617/

Billingham, & Armes, 1999) have been polymerized by CRP in aqueous media. Because of this progress in the CRP technique, we can avoid the two-step reaction: polymerization of protected monomers and deprotection of grafted polymers, though the polymerization mechanism of the CRP is under debate (Konkolewicz et al., 2014; Percec et al., 2006; Rosen & Percec, 2009). Besides, HA-based brush copolymers were successfully synthesized through the synthesis of HA-based macroinitiators and the subsequent CRP of various monomers (Pitarresi, Fiorica, Licciardi, Palumbo, & Giammona, 2013). Utilizing these CRP techniques allows us to prepare HA-*g*-PAA by a one-step polymerization of sodium acrylate.

In addition, PAA has abundant carboxyl groups and is well known as forming insoluble salts with multivalent ions such as Ca^{2+}. This conformational change of PAA has been energetically studied (Huber, 1993; Schweins & Huber, 2001), where PAA changes from a random coil to a compact spherical shape through a pearl-necklace-like intermediate, while HA is known not to form an insoluble calcium salt (Chang & Boackle, 1985; Gabriel & Carr, 1989). Thus, HA-*g*-PAA can form a gel-like insoluble salt compared with the hydrophobic insoluble calcium salt of PAA because of the high water content of the partially unmodified HA units of HA-*g*-PAA. In addition, the calcium salt of HA-*g*-PAA is expected to be a new biodegradable and biocompatible material to form an insoluble salt *in situ* by simultaneous injection and mixing of aqueous HA-*g*-PAA and $CaCl_2$ solution as in a fibrin sealant system (Ahmed, Dare, & Hincke, 2008), where fibrinogens are enzymatically gelled by mixing with thrombin and $CaCl_2$. Because HA-*g*-PAA can form an insoluble salt without reactive group modification, nonspecific reaction with cells/tissues would be avoided, and thus high biocompatibility is expected.

In this study, PAA was, for the first time, grafted from the HA backbone *via* CRP in aqueous media. The formation of an insoluble calcium salt as a result of the binding between HA-*g*-PAA and Ca^{2+} was investigated. The degradation behavior and biocompatibility to mesothelial and fibroblast cells of HA-*g*-PAA were assessed *in vitro*. Finally, HA-*g*-PAA and its calcium salt were administered subcutaneously and intraperitoneally, and evaluated *in vivo*.

2. Materials and methods

2.1. Materials

HA (FCH200, M_w = 2.0 MDa, for polymer synthesis, and FCH80, M_w = 0.8 MDa, for viscosity measurement) was kindly donated by Kikkoman Biochemifa Co. (Tokyo, Japan). Tetrabutylammonium hydroxide (TBA), triethylamine, 2-bromoisobutyryl bromide, copper(I) bromide (CuBr), sodium acrylate, polyacrylic acid sodium salt (PAA; Polymerization Degree 2700–7500), dimethyl sulfoxide (DMSO), *N*,*N*,*N*′,*N*″,*N*″-pentamethyldiethylenetriamine (PMDETA), tetrahydrofuran (THF), sodium chloride (NaCl), and lipase from *Pseudomonas cepacia* (Lipase PS) were purchased from Wako (Osaka, Japan). Dialysis membrane (Spectra/Por, MWCO = 6–8 kDa) was purchased from Spectrum Laboratories Inc. (Rancho Dominguez, CA, USA). Cation-exchange resin (DOWEX 50WX8) and hyaluronidase (HAse) from bovine testes (Type I-S, lyophilized powder, 400–1000 unit/mg solid) were purchased from Sigma-Aldrich (St. Louis, MO, USA). A double-barrel syringe was kindly donated by Baxter (Deerfield, IL, USA).

2.2. Characterization

^{1}H NMR measurements were carried out on an ALPHA FT-NMR spectrometer (500 MHz) αJEOL JNM-A500 (JEOL, Tokyo, Japan) using D_2O as a solvent. FT-IR spectra were obtained using the potassium bromide disk method on an FT/IR-4200ST spectrometer (JASCO, Tokyo, Japan). Viscosity was measured using a TVE-22 cone-type viscometer (Toki Sangyo, Tokyo, Japan). Molecular weight distributions were measured using gel permeation chromatography (GPC) equipped with an LC-10AD$_{VP}$ pump (Shimadzu, Tokyo, Japan) and an 830-RI differential refractive index detector (JASCO, Tokyo, Japan), which was set at 35 °C. Separation was carried out at room temperature with a TSK-Gel GMPW$_{XL}$ column (TOSOH, Tokyo, Japan) at a flow rate of 0.5 mL/min, and sodium phosphate buffer (pH 6.7) containing 0.05 M phosphate buffer and 0.2 M NaCl was used as the eluent. The molecular weights were determined relative to dextran standards (Extrasynthese, Genay, France). Carbazole assay (Bitter & Muir, 1962) was conducted using HA solutions of known concentrations as standards (La Gatta et al., 2013; Yeo et al., 2006b; Shu, Liu, Palumbo, Luo, & Prestwich, 2004). The residual copper content of the product was measured using a Z-2000 atomic absorption spectrometry (Hitachi High-Technologies Corporation, Tokyo, Japan).

2.3. Synthesis of 2-bromoisobutyryl hyaluronic acid (HA–Br)

HA (0.994 g) was dissolved in distilled water (300 mL), subsequently changing Na^+ to H^+ using a cation-exchange resin. The resin was removed by filtration, and TBA (7.1 mL, 10% aqueous solution) was added and stirred at room temperature for 2 h. Then, the aqueous tetrabutylammonium HA (HA–TBA) was lyophilized.

HA–TBA (1.20 g) was dissolved in a mixture of THF (24.0 mL) and DMSO (12.0 mL). After adding triethylamine (1.62 mL), 2-bromoisobutyryl bromide (0.95 mL) was added dropwise at 0 °C. The solution was stirred for 1 h at room temperature. After that, the white precipitate was filtered and dissolved in water. The solution was dialyzed against aqueous sodium chloride solution and distilled water, and then lyophilized (yield 39.8%).

2.4. Synthesis of HA grafted with PAA (HA-g-PAA), polymerization of sodium acrylate

HA–Br (190 mg), sodium acrylate (5.00 g), and PMDETA (444 μL) were dissolved in distilled water (20.0 mL) in a Schlenk flask. The solution was degassed by three freeze–pump–thaw cycles, and then CuBr (153 mg) was added after purging with nitrogen, and the solution was degassed again using a freeze–pump–thaw cycle. The polymerization reaction was performed at 25 °C for 45 h. The obtained polymer was dialyzed against distilled water for 3 days. After we confirmed that the electric conductivity (an indicator of the amount of impurities) of the dialysis fluid was at the same level with that of distilled water, the polymer solution was lyophilized. The residual copper content was 0.04 wt%. The reaction yield was 83.1% (Fig. 1).

2.5. Evaluation of the degradation behavior of HA-g-PAA by HAse and/or Lipase

HA-*g*-PAA (1.0 mg) was dissolved in 1.0 mL of sodium phosphate buffer (pH 6.7) containing 0.05 M phosphate buffer and 0.2 M NaCl. Then, HAse (10 unit/mL) and/or lipase (10 unit/mL) was added. The solution with or without the enzymes was then incubated at 37 °C for a week. The molecular weight distributions of HA-*g*-PAA before and after incubation were measured by GPC as described in Section 2.2.

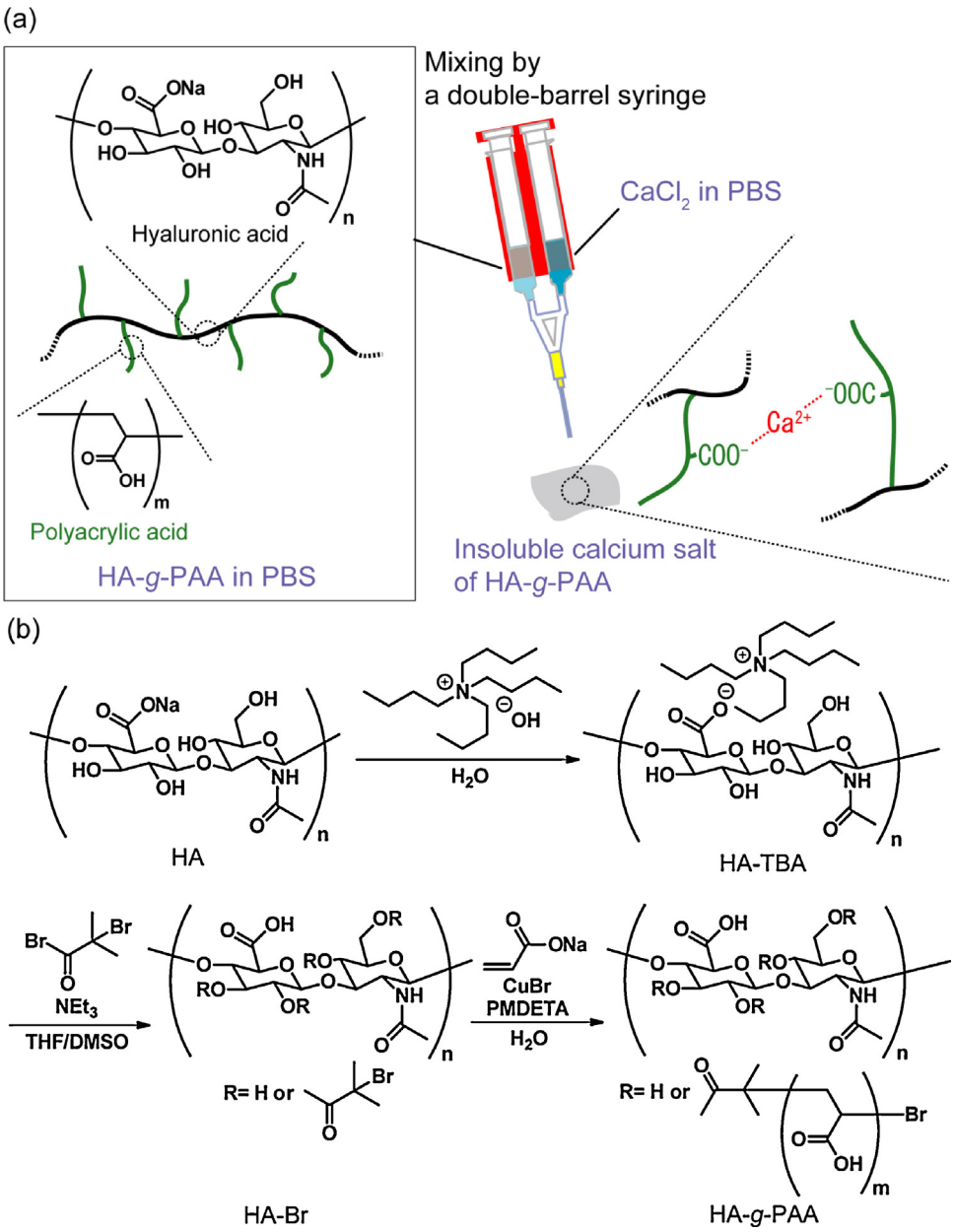

Fig. 1. (a) Schematic illustration of hyaluronic acid grafted with polyacrylic acid (HA-*g*-PAA) and formation of an insoluble calcium salt of HA-*g*-PAA. (b) Synthetic route to HA-*g*-PAA.

2.6. Evaluation of the insoluble calcium salt formation of HA-g-PAA

Optical transmittance of HA-*g*-PAA solution (1.0 wt%) at different $CaCl_2$ concentration (0–45 mM) were measured by a V-630BIO UV–vis spectrometer (JASCO, Tokyo, Japan) at 500 nm. Decrease in transmittance, caused by light scattering from insoluble salts, was used as an indicator of the insoluble salt formation. Normal saline was used as a solvent.

2.7. Cell viability assay of HA-g-PAA and its calcium salt

In vitro cell viability in the presence of HA-*g*-PAA was determined by MTT assay (Cell Titer 96; Promega, Madison, WI, USA) using a human mesothelial cell line (MeT-5A (CRL-9444); ATCC, Manassas, VA, USA) and a mouse fibroblast cell line (NIH-3T3; Riken Cell Bank, Tsukuba, Japan).

Mesothelial cells were grown and maintained in complete growth medium (Medium199 with Earle's BSS, 0.75 mM L-glutamine and 1.25 g/L sodium bicarbonate supplemented with 3.3 nM epidermal growth factor, 400 nM hydrocortisone, 870 nM insulin, 20 mM HEPES, and 10% fetal bovine serum (FBS)) at 37 °C in 5% CO_2. Mesothelial cells were seeded in a 96-well plate at an initial density of *ca.* 5000 cells/well and incubated at 37 °C in 5% CO_2 overnight. The medium was replaced with media containing different concentrations of HA-*g*-PAA. On the second day after adding the materials, the MTT assay was performed. Tetrazolium salt solution (15 μL) was added to each well and incubated at 37 °C for 4 h. The purple formazan produced by active mitochondria was solubilized using detergent solution (100 μL/well), and then the absorbance at 570 nm was measured using a plate reader (2030

ARVO V3; PerkinElmer, Waltham, MA, USA). The absorbance values were normalized to wells where no test materials were added to the media. In the case of fibroblast cells, DMEM with 10% FBS was used as the medium. Other procedures were the same as in the case of mesothelial cells.

In vitro cell viability in the presence of the calcium salt of HA-*g*-PAA was also determined by MTT assay using a human mesothelial cell line and a mouse fibroblast cell line. Cells were prepared in the same way. Phosphate buffer saline (PBS) containing HA-*g*-PAA (50 μL) and PBS containing $CaCl_2$ (50 μL) were mixed, and the mixture was centrifuged at 10,000 rpm for 3 min. Supernatant was removed by pipetting, and the obtained calcium salt of HA-*g*-PAA was applied to seeded cells on a 96-well plate. On the second day after adding the materials, the medium was replaced with a fresh medium. Then, the MTT assay was performed in the same manner.

2.8. Subcutaneous and intraperitoneal administration of the calcium salt of HA-g-PAA using a double-barrel syringe

The experiments were performed at the Animal Research Section, Center for Disease Biology and Integrative Medicine, Faculty of Medicine, the University of Tokyo. The Animal Care Committee of the University of Tokyo approved all procedures in this study before it began.

ICR mice (3 week old, male) weighing 20 g were purchased from CLEA Japan, Inc. (Tokyo, Japan) and housed in groups in a 6 am–6 pm light–dark cycle. The polymer was sterilized by UV irradiation for 2 h and then dissolved in PBS at 2 wt% concentration. Anesthesia was induced with 50 mg/kg ketamine and 10 mg/kg xylazine.

PBS containing HA-*g*-PAA (2 wt%, 0.5 mL) was administered intraperitoneally using a syringe and a 24 ga needle (Terumo, Tokyo, Japan). In addition, PBS containing HA-*g*-PAA (2 wt%, 0.5 mL) and PBS containing $CaCl_2$ (1 wt%, 0.5 mL) were injected subcutaneously to the posterodorsal wall and intraperitoneally using a dual syringe applicator.

The mice treated by subcutaneous administration were sacrificed 1 day, 3 days, and 1 week after the injections ($N = 1$), and the residue of the materials was sampled and fixed in 10% formalin, and processed for histology (hematoxylin–eosin (HE)-stained slides) using standard techniques. The mice treated by intraperitoneal administration were sacrificed 1 week after the injections, and the presence of residue and adhesions was evaluated ($N = 3$). Abdominal contents were sampled, fixed in 10% formalin, and processed for histology (HE-stained slides) using standard techniques.

3. Results and discussion

3.1. Synthesis and characterization of HA-g-PAA

Because 2-bromoisobutyryl bromide did not dissolve in water, the sodium ion of HA was exchanged by TBA so that HA became solubilized in organic solvents. After that, synthesis of HA–Br, which was a HA-based macroinitiator, was performed by transforming the hydroxyl groups of HA–TBA into 2-bromoisobutyryl groups in the mixture of THF and DMSO. Synthesis of HA–TBA was confirmed by ^{1}H NMR and FT-IR (Figs. 2 and 3a). The ^{1}H NMR spectrum of HA–TBA showed large peaks from TBA (δ (ppm) (DMSO-d_6), 0.93 (*t*, 12H), 1.34 (*sext*, 8*H*), 1.63 (*quin*, 8*H*), 3.18 (*t*, 8*H*)) as well as the characteristic peak from methyl protons of *N*-acetyl-D-glucosamine at 2.01 ppm (substitution ratio: 224%). In addition, the FT-IR spectrum of HA–TBA showed characteristic peaks from HA at 1200–900 cm^{-1}, which were overlapped by ν_{as}(C—O—C) from glycosidic bonds at about 1150 cm^{-1}, and absorption bands of ν(C—O), ν(C—C), and δ(C_1—OH) from monosaccharide units (Gilli, Kacurakova, Mathlouthi, Navarini, & Paoletti, 1994; Hrabarova et al., 2012; Kacurakova, Capek, Sasinkova, Wellner and Ebringerova, 2000). We also found that the FT-IR spectrum of HA–TBA showed the increase in the peaks around 3000–2800 cm^{-1} compared to that of native HA. These peaks were assigned to the absorption bands of ν(C—H) of methyl and methylene groups, both of which were abundant in TBA. Synthesis of HA–Br was also confirmed by ^{1}H NMR and FT-IR (Figs. 2 and 3a). Protons from the 2-bromoisobutyryl groups were confirmed at 1.27 ppm in the ^{1}H NMR spectrum, while the FT-IR spectrum of HA–Br showed characteristic peaks from HA, as explained above. The degree of modification was calculated from the ^{1}H NMR spectra by the ratio of the area of the peak for methyl groups of *N*-acetyl-D-glucosamine (at 2.01 ppm) to that for 2-bromoisobutyryl groups (at 1.27 ppm); the degree of bromine modification was 48.0%.

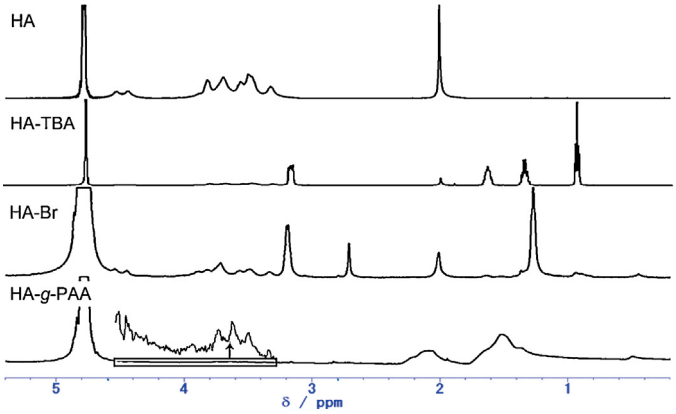

Fig. 2. ^{1}H NMR spectra of HA, HA–TBA, HA–Br, and HA-*g*-PAA in D_2O.

Using HA–Br as a macroinitiator, the polymerization of sodium acrylate was performed *via* CRP in aqueous media. The ^{1}H NMR spectrum of HA-*g*-PAA (Fig. 2) showed the appearance of new broad peaks at 1.0–1.8 and 1.8–2.4 ppm that were assigned to the α-protons and β-protons at PAA, respectively. In addition, the peaks assigned as the HA backbone were still confirmed at 3.3–4.1 and 4.4–4.6 ppm. The FT-IR spectrum of HA-*g*-PAA (Fig. 3a) also showed peaks characteristic of PAA at 1560 cm^{-1} and 1411 cm^{-1}, which are due to ν_{as}(O—C—O) and ν_s(O—C—O) of the carboxylic anions, respectively. It also showed the characteristic peaks of HA at 1200–900 cm^{-1}, especially at about 1150 cm^{-1}, which reflected the stretching ν_{as}(C—O—C) of the glycosidic bonds. The weight ratio of the HA backbone to the HA-*g*-PAA polymer was determined to be 3.5 wt% by carbazole assay. Using this weight ratio (3.5 wt%) as well as the degree of bromine modification of HA–Br (48.0%), the chemical structure of HA-*g*-PAA can be estimated as follows; two PAA chains (*ca.* 5.5 kDa) were grafted from a HA repeating unit (379 Da).

We measured the molecular weight distributions of HA, HA–TBA, HA–Br, and HA-*g*-PAA using GPC relative to dextran standards (Fig. 3b). The resulting weight-average molecular weights (M_ws) of HA, HA–TBA, HA–Br, and HA-*g*-PAA were 2.0×10^7, 3.0×10^6, 2.3×10^4, and 9.8×10^5, respectively. After the TBA substitution, the molecular weight distribution shifted to lower molecular weights. This result suggests that HA backbone was partially degraded during TBA substitution, which would be due to pH increase caused by TBA addition. In fact, the cleavage of the HA chain into short oligosaccharide segments during the ion-exchange procedure from HA to HA–TBA was reported in a previous study (Mortisen, Peroglio, Alini, & Eglin, 2010). In addition, as a result of the subsequent bromine modification, the molecular weight decreased further and the resulting molecular weight distribution of HA–Br was bimodal. The pH increase caused by the excess triethylamine used in the bromine modification would be a reason for the further degradation of HA. Consequently, molecular weight

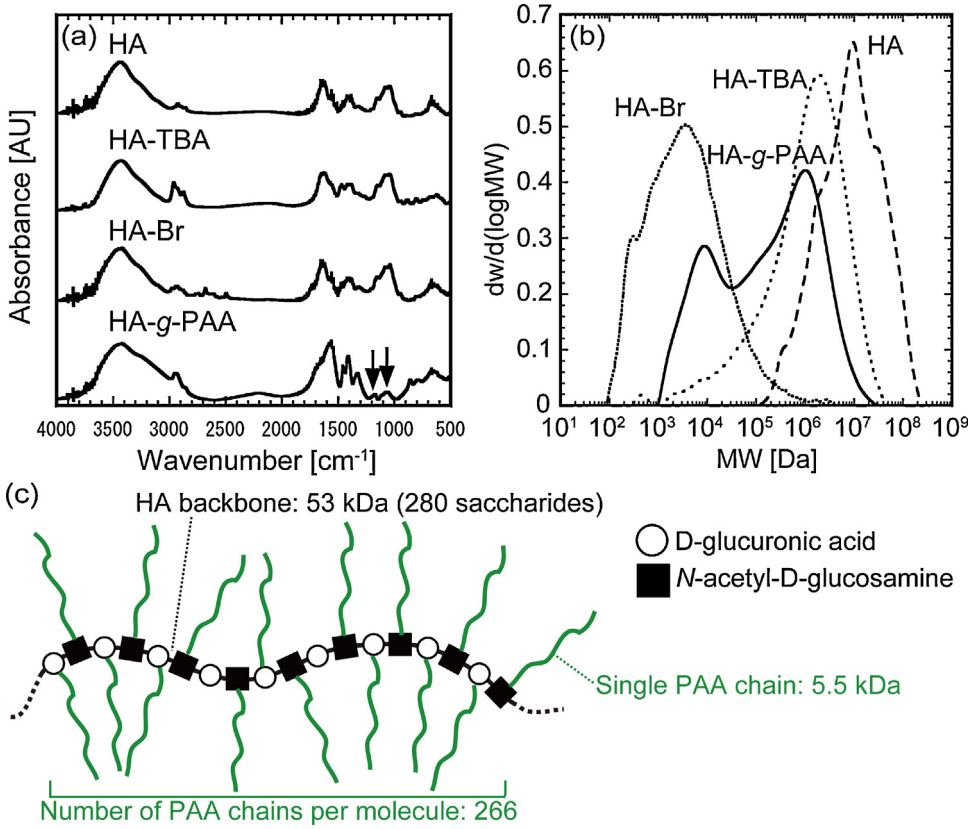

Fig. 3. (a) FT-IR spectra of HA, HA–TBA, HA–Br, and HA-*g*-PAA. The arrows indicate the characteristic peaks of HA. (b) Molecular weight distributions of HA ($M_w = 2.0 \times 10^7$, $M_n = 2.9 \times 10^6$, $M_w/M_n = 7.1$), HA–TBA ($M_w = 3.0 \times 10^6$, $M_n = 4.6 \times 10^4$, $M_w/M_n = 65.9$), HA–Br ($M_w = 2.3 \times 10^4$, $M_n = 1.1 \times 10^3$, $M_w/M_n = 21.7$), and HA-*g*-PAA ($M_w = 9.8 \times 10^5$, $M_n = 1.7 \times 10^4$, $M_w/M_n = 56.9$). (c) Schematic structure of the HA-*g*-PAA main products.

distribution of HA-*g*-PAA after polymerization showed bimodal distribution as shown in Fig. 3b; one peak is around 1000 kDa and the other is 10 kDa. We consider that the former peak corresponds to HA-*g*-PAA polymers, while the latter peak corresponds to low molecular weight fragments of HA-*g*-PAA derived from the low molecular weight HA–Br fragments (around 0.3 kDa). The M_w of the HA-*g*-PAA main products (above 60 kDa; 70 wt%) was 1.5×10^6, and thus the M_w of the HA backbones in the HA-*g*-PAA polymers was calculated to be 5.3×10^4 (corresponds to *ca.* 280 saccharides), considering that the weight ratio of the HA backbone to the HA-*g*-PAA polymer was 3.5 wt% as mentioned above (Fig. 3c).

PAA grafting affected the viscosity of HA. We measured the viscosity of HA-*g*-PAA using a viscometer (shear rate was fixed at 40 s^{-1}). For comparison, the viscosity of HA, M_w of which was similar to that of HA-*g*-PAA, was also measured. As a result, the viscosity of HA-*g*-PAA solution (1 wt% in PBS) was 10 mPa s, while that of HA solution ($M_w = 0.8$ MDa, 1 wt% in PBS) was 1.7×10^2 mPa s. These results indicate that PAA grafting dramatically decreased the viscosity of HA, which is an advantage for injection materials. The decrease of HA viscosity by chemical modification of HA has also been previously reported. It was pointed out that the decrease in viscosity was due to the disruption of the hydrogen bonds by steric hindrance of the modified groups (Schanté, Zuber, Herlin, & Vandamme, 2012). Therefore, in our case, it was also reasonable to assume that HA-*g*-PAA had lower viscosity than native HA because intra- and/or intermolecular hydrogen-bond formation of HA-*g*-PAA was prevented by steric hindrance of the grafted PAA. The disruption of intra- and/or intermolecular hydrogen bonds of HA-*g*-PAA would make the polymer chains more flexible than native HA (Hardingham, 2004), which enhances the sphere-like behavior in media and reduces entanglements between polymer chains, thus decreasing the viscosity of HA-*g*-PAA.

3.2. Degradation behavior of HA-g-PAA by enzymes

When used for medical applications (*e.g.*, drug delivery in the peritoneum and materials preventing peritoneal adhesion), degradation behavior in the physiological environment is quite important. We incubated HA-*g*-PAA with enzymes HAse and/or lipase, both of which are abundantly contained in our body fluid, to examine the degradation behavior of HA-*g*-PAA under simulated physiological conditions. Degradation of HA-*g*-PAA was characterized by changes in molecular weight distributions before and after incubation at 37 °C for a week, measured by GPC (Fig. 4).

The degradation and metabolism of native HA has been studied in detail, and it has been reported that HA is degraded quickly by HAses (Lepperdinger, Fehrer, & Reitinger, 2004). Fig. 4b shows the degradation behavior of HA-*g*-PAA in the presence of HAse (10 unit/mL). The M_w of HA-*g*-PAA decreased by 40% after the incubation as a result of the degradation of the HA backbone in HA-*g*-PAA. This degradation rate is much slower than in native HA; M_w of native HA (4 mg/mL) was reported to be decreased by 93% in just 60 min of incubation at 37 °C in the presence of HAse (10 unit/mL) (Gatta, De Rosa, Marzaioli, Busico, & Schiraldi, 2010), while that of HA-*g*-PAA decreased by only 40% even after incubation for a week, as shown in Fig. 4b. The effects of HA modification on its degradation behavior have been investigated in previous studies; in the case of HA esters (Zhong et al., 1994) and amino acid-modified HA (Schanté, Zuber, Herlin, & Vandamme, 2011; Schanté et al., 2012), degradation of modified HA by HAse was slower than native HA, and the decrease in the enzymatic degradation was proportional to the degree of modification. Hence, we assume that degradation of HA-*g*-PAA by HAse was inhibited by grafted PAA. Steric hindrance by grafted PAA would inhibit the diffusion and biological recognition of HAse, which results in the slower degradation of HA-*g*-PAA than

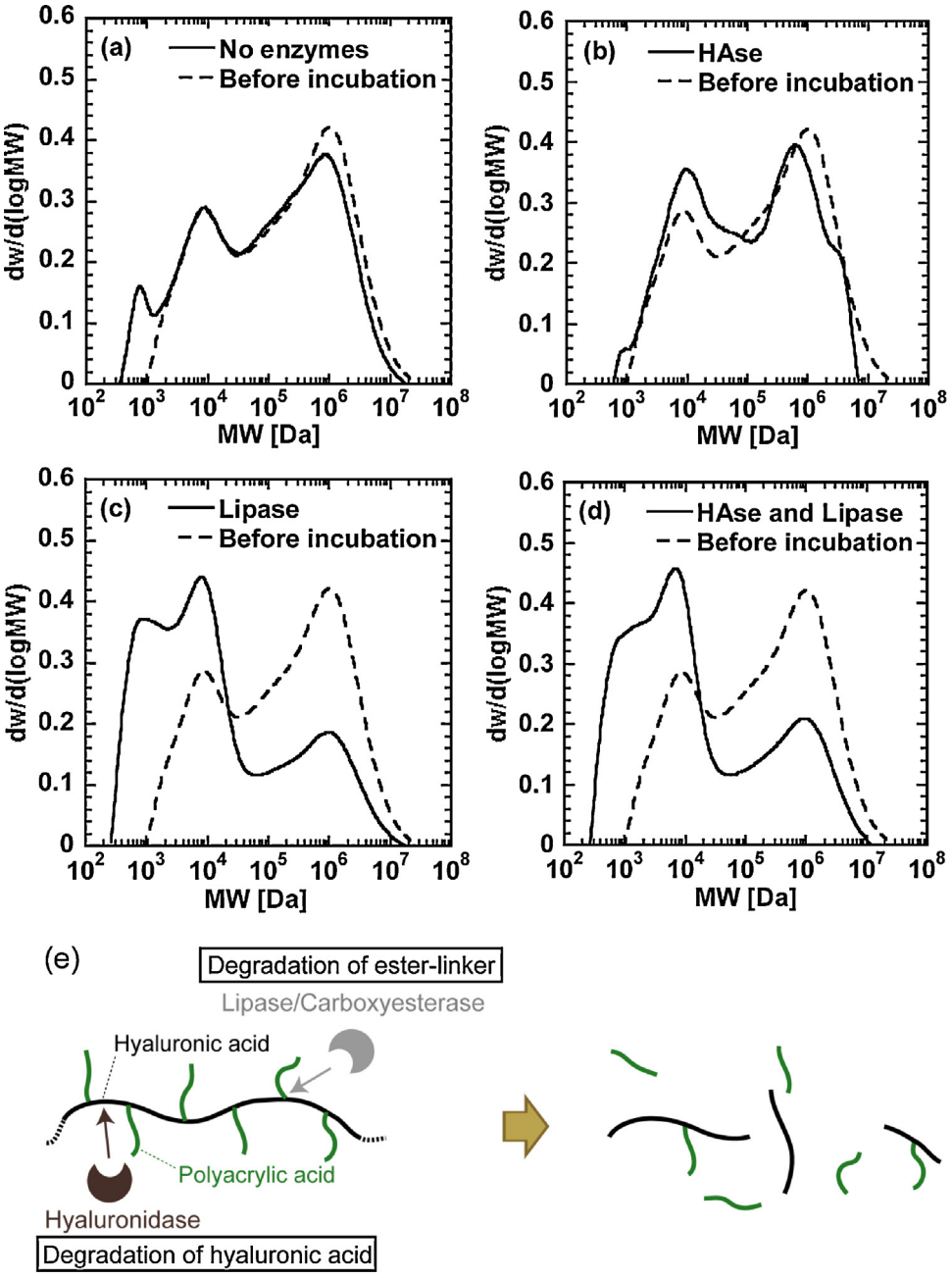

Fig. 4. Degradation behavior of HA-*g*-PAA at 37 °C in sodium phosphate buffer that contained different enzymes: (a) no enzymes, (b) 10 unit/mL of HAse, (c) 10 unit/mL of lipase, and (d) a mixture of 10 unit/mL of HAse and lipase. (e) Schematic illustration of the degradation of HA-*g*-PAA.

native HA. The slow degradation rate of the HA backbone would provide a way to prolong the retention time of HA-*g*-PAA in the human body for future medical applications.

While HA can be completely degraded and metabolized in our body, grafted PAA cannot be degraded. Thus, grafted PAA chains should be detached from the HA backbone and excreted from the kidneys. Because we grafted relatively short PAA chains *via* ester bonds from the HA backbone, PAA chains were expected to be detached by lipase, an enzyme that degrades ester bonds *via* hydrolysis, and then excreted from the kidneys. In a previous research, nanoparticles of dextran substituted with decanoate esters showed degradation in the presence of lipase; highly substituted dextran esters were degraded by lipase, which lowered the degree of substitution and then enabled further degradation by both lipase and dextranase (Kaewprapan, Inprakhon, Marie, & Durand, 2012). In the same way, highly grafted HA-*g*-PAA might also degrade by detaching PAA chains in the presence of lipase, which would then enable the degradation of the HA backbone by HAse. Fig. 4c shows the degradation behavior of HA-*g*-PAA in the presence of lipase. Approximately 70 wt% of HA-*g*-PAA had molecular weights under 60 kDa after incubation with lipase. The M_w calculated from the main peak (under 60 kDa) in molecular weight distribution of HA-*g*-PAA after the incubation (Fig. 4c) was 8.03×10^3. This M_w coincided with a molecular weight of each grafted PAA chain estimated by calculating the ratio of the total weight of grafted PAA chains to the number of moles of bromine modified to HAs as discussed in Section 3.1 (*ca.* 5.5 kDa), suggesting that grafted PAA chains were detached from HA by hydrolysis and enzymatic degradation. In addition, the molecular weights of detached PAA chains were low enough to be excreted from the kidneys, because the threshold M_w for kidney

excretion is reported to be *ca.* 60 kDa (Brenner, Hostetter, & Humes, 1978; Yamaoka, Tabata, & Ikada, 1994). These results indicate that grafted PAA chains had the potential to be detached from HA and finally excreted from the kidneys.

Even in the presence of both HAse and lipase, the result was consistent with those in the presence of only HAse or lipase. Enzymatic degradation of the HA backbone by HAse was inhibited by grafted PAA, while grafted PAA was detached by hydrolysis and enzymatic degradation by lipase to the degree that *ca.* 70 wt% of HA-*g*-PAA had molecular weights under 60 kDa, which were low enough to be excreted from the kidneys (Fig. 4d). Because both HAse and lipase/carboxyesterase are contained abundantly in our body fluids, similar results are expected even when injected *in vivo*.

In our experiment, while degradation of HA by HAse was inhibited by steric hindrance of the grafted PAA chains, lipase could detach PAA chains *via* hydrolysis of ester bonds, which are located at the bottom of the PAA chains. This difference in HA-*g*-PAA degradation behavior between HAse and lipase was presumably attributable to a wider substrate specificity of lipase than HAse. Lipase can hydrolyze not only triacylglycerol but also various kinds of ester bonds, while HAse can hydrolyze only the β-1,4 glycosidic linkage between *N*-acetylglucosamine and glucuronate of HA. Therefore, steric hindrance of PAA chains would affect the biological recognition of HAse more significantly than that of lipase. This prolonged degradation of the HA backbone and scission of the grafted PAA chains of HA-*g*-PAA would enable kidney excretion and good biocompatibility for medical applications.

3.3. Formation of a calcium salt of HA-g-PAA

HA-*g*-PAA solution formed an insoluble salt suspension within a second when mixed with Ca^{2+} ions. The insoluble salt was then gradually precipitated in the solution obtaining a solid material, and this solid material can be re-dissolved by exchanging ions from Ca^{2+} to Na^{+} (Fig. 5a). Fig. 5b shows optical transmittances of the mixture solution of HA-*g*-PAA (1.0 wt%) and $CaCl_2$ as a function of Ca^{2+} concentration (0–45 mM). When the concentration of Ca^{2+} ions was less than 20 mM, the mixture was almost transparent. On the other hand, when the concentration of Ca^{2+} ions was 20 mM or above, the initially transparent solution became cloudy immediately after mixing with $CaCl_2$, which corresponded to the formation of insoluble salt. Threshold calcium concentration (around 20 mM) was observed in the insoluble salt formation of HA-*g*-PAA. These trends were similar with the result of linear PAA (triangles in Fig. 5b). It was reported that linear PAA forms insoluble calcium salt by bridging of carboxyl groups through Ca^{2+} ions and/or hydrophobic interaction of PAA chains through Ca^{2+}-induced coil collapse (Huber, 1993; Schweins & Huber, 2001). Therefore, HA-*g*-PAA would also form insoluble salt with Ca^{2+} ions in the same manner. In addition, it was also found that the threshold Ca^{2+} concentration to induce insoluble salt formation of HA-*g*-PAA was larger than that of linear PAA. This difference would be due to the high water content of HA units of HA-*g*-PAA. The abundant hydroxyl and carboxyl groups of HA units would increase the hydrophilicity of the HA-*g*-PAA polymer. Thus, compared with native PAA, more Ca^{2+} ions were needed to increase the overall hydrophobicity of calcium salt of HA-*g*-PAA for inducing precipitation. Because this insoluble salt formation occurs immediately after mixing with $CaCl_2$ solution, and the obtained insoluble salt can have high water content compared with the hydrophilic insoluble salt of native PAA, HA-*g*-PAA is expected to become a novel *in situ* cross-linking material.

3.4. Biocompatibility of HA-g-PAA and its calcium salt in vitro

In previous researches, various kinds of *in situ* cross-linkable hydrogels composed of HA have been reported by utilizing HA

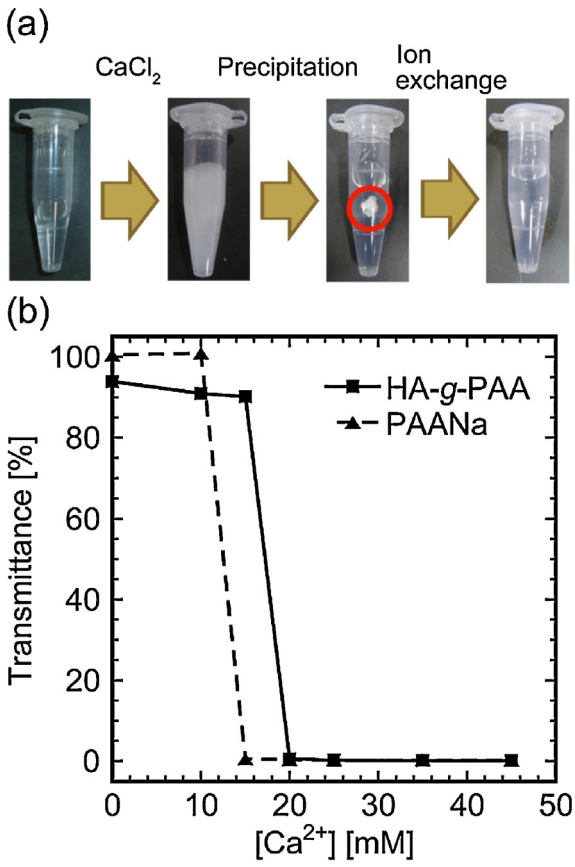

Fig. 5. (a) Formation of the insoluble salt suspension of HA-*g*-PAA, following precipitation of the insoluble salt, and the re-dissolution of the insoluble salt by ion exchange. (b) Transmittances of HA-*g*-PAA (squares) and PAA (triangles) solution at different Ca^{2+} concentration. The polymer concentration was fixed at 1.0 wt%. Normal saline was used as a solvent.

modified with reactive groups. These reactive groups, however, cause a nonspecific reaction with tissue, and thus a relatively high cytotoxicity of the precursor polymers was inevitable. In the case of HA-*g*-PAA, lower cytotoxicity was expected because such reactive groups were not modified. The effect of HA-*g*-PAA solution on fibroblast (NIH-3T3) and mesothelial cell (MeT-5A) viability after two days' incubation was revealed by MTT assay in terms of the mitochondrial function (Fig. 6a). Cell viability of both NIH-3T3 and MeT-5A was not significantly affected when the concentration of HA-*g*-PAA was below 0.2 wt%, although the viability of NIH-3T3 decreased above 0.5 wt%. Thus, it can be concluded that HA-*g*-PAA solution had sufficient biocompatibility comparable to native HA solution, especially to mesothelial cells, as an injection material.

When aiming at utilizing the HA-*g*-PAA insoluble salt as an injection material, it is also important to evaluate the biocompatibility of the insoluble salt, because the results might be greatly different between HA-*g*-PAA precursor polymers and the calcium salt. Hence, the effect of the insoluble salt on fibroblast and mesothelial cell viability was also investigated. In this experiment, the concentration of HA-*g*-PAA was varied from 0.1 wt% to 1 wt%, the same range as in Fig. 6a, while the Ca^{2+} concentration was fixed at 0.5 wt%. Since the insoluble salts are supposed to precipitate and become a solid form after injected into body as mentioned in Section 3.3, we consider that biocompatibility of the insoluble salts in a solid form, rather than suspension, is important. Thus, the insoluble salt of HA-*g*-PAA was applied to cells as pellets, which was obtained by centrifugation. The cell viability of both NIH-3T3 and MeT-5A after

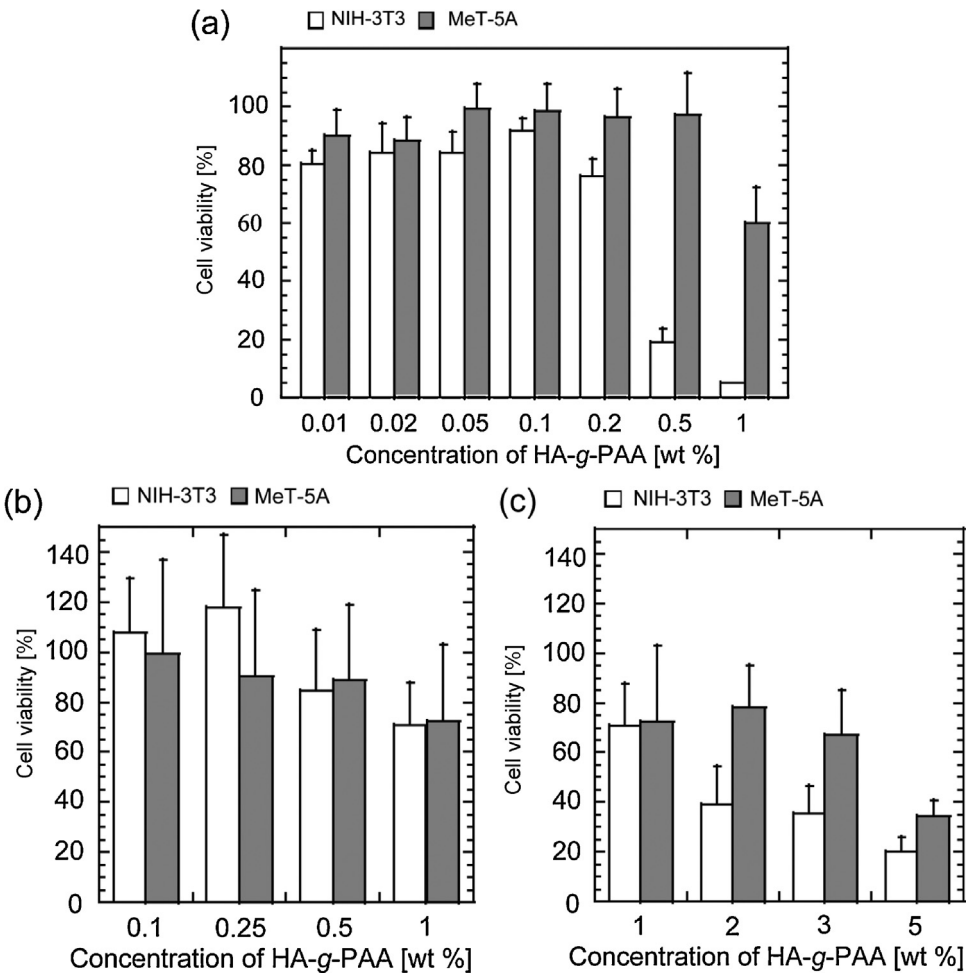

Fig. 6. Effect of HA-*g*-PAA and its insoluble calcium salt on fibroblast and mesothelial cell viability measured by MTT assay after two days' incubation. Data are averages ± standard deviations ($N = 8$). (a) HA-*g*-PAA without Ca^{2+}. (b) Insoluble calcium salts of HA-*g*-PAA. Ca^{2+} concentration was fixed at 0.5 wt%, while HA-*g*-PAA concentration was changed between 0.1 and 1 wt%. (c) Insoluble calcium salts of HA-*g*-PAA. The weight ratio of HA-*g*-PAA to $CaCl_2$ was fixed at 2:1.

incubation with the insoluble salt of HA-*g*-PAA was higher than that with HA-*g*-PAA solution (Fig. 6b). Similar phenomena were also reported in another study, in which *in situ* cross-linkable hydrogels composed of HA showed no apparent local toxicity *in vivo*, although the precursor polymers themselves showed some toxicity. The rapid cross-linking of precursor polymers left few free precursors that induced cytotoxicity, which resulted in low cytotoxicity (Ito et al., 2007b). Thus, the reason for the lower cytotoxicity of the insoluble salt of HA-*g*-PAA than its precursor polymers in our case would be almost the same; the concentration of free HA-*g*-PAA polymer in culture media remained low by forming the insoluble calcium salt.

Because the insoluble salt with 1.0 wt% of HA-*g*-PAA and 0.5 wt% of $CaCl_2$ did not show significant cytotoxicity, we fixed the composition of HA-*g*-PAA/$CaCl_2$ at this ratio and further examined the dose dependency by increasing the mass of insoluble salt (Fig. 6c). The results showed that in the case of mesothelial cells, insoluble salts with as high as 3 wt% of HA-*g*-PAA did not significantly affect the cell viability, while in the case of fibroblast, an apparent decrease of cell viability was observed when insoluble salts with more than 1 wt% of HA-*g*-PAA were used. According to these results, we set the concentration of HA-*g*-PAA and $CaCl_2$ solutions at 1 wt% and 0.5 wt%, respectively, for the following *in vivo* injection experiments.

3.5. *In vivo* biocompatibility of the calcium salt of HA-*g*-PAA by subcutaneous injection

The calcium salt of HA-*g*-PAA was administered subcutaneously to three mice, and each mouse was evaluated 1, 3, and 7 days after the injections. Although *N* was just one for each condition

Table 1
Evaluation of material residue and adhesion formation after subcutaneous or intraperitoneal injection of the insoluble calcium salt of HA-*g*-PAA in mice.

Material	Administration route	Postoperative day [days]	Body weight gain postoperatively [%]	Material residue	Peritoneal adhesion
Calcium salt of HA-*g*-PAA[a]	Subcutaneously	1	0.3	1/1	–
Calcium salt of HA-*g*-PAA[a]	Subcutaneously	3	9.4	1/1	–
Calcium salt of HA-*g*-PAA[a]	Subcutaneously	7	13.9	1/1	–
HA-*g*-PAA[b]	Intraperitoneally	7	17.0 ± 1.8	0/3	0/3
Calcium salt of HA-*g*-PAA[a]	Intraperitoneally	7	17.0 ± 1.9	2/3	0/3

[a] The calcium salt of HA-*g*-PAA was a mixture of 2 wt% of HA-*g*-PAA and 1 wt% of $CaCl_2$, this mixture being administered using a double-barrel syringe. The administration volume was 1.0 mL, which was the sum of 0.5 mL of HA-*g*-PAA solution and 0.5 mL of $CaCl_2$ solution.
[b] HA-*g*-PAA was at a concentration of 2 wt% in PBS. The administration volume was 0.5 mL.

as shown in Table 1, all of the mice showed a weight gain with the increase in postoperative days and showed a healthy condition. HA-*g*-PAA calcium salts formed a disk-shaped material residue under their dermis, as shown in Fig. 7a and b. Moreover, the HE-stained picture in Fig. 7c shows a similar inflammation response to previously reported HA-based materials (Bulpitt & Aeschlimann, 1999; Ito et al., 2007a). Because of this positive subcutaneous result, we administered the materials intraperitoneally.

3.6. *In vivo* biocompatibility of HA-*g*-PAA and its calcium salt in the peritoneum

None of the mice generated peritoneal adhesion by intraperitoneal administration of HA-*g*-PAA or its insoluble calcium salt, as shown in Table 1.

When HA-*g*-PAA was administered without $CaCl_2$, HA-*g*-PAA was completely cleared from the peritoneum one week after injection. We observed no pathological appearance, including the formation of peritoneal adhesions. Although some materials such as chitosan and its derivatives (Yeo et al., 2006a) have been reported to cause the formation of adhesions, HA-*g*-PAA and its calcium salt showed good biocompatibility, like chemically unmodified HA in

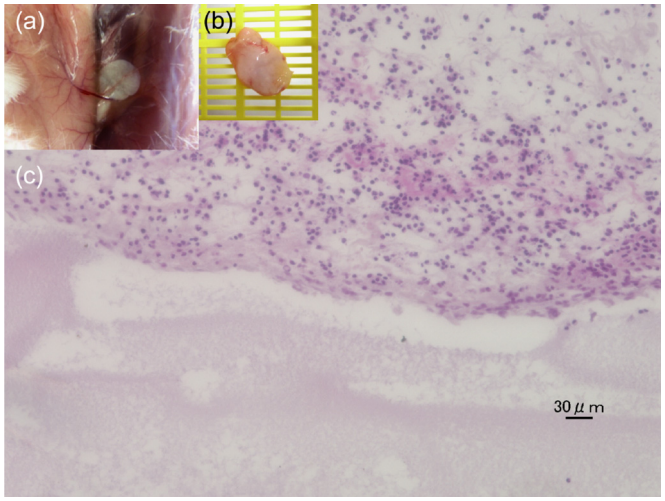

Fig. 7. Subcutaneously administered insoluble calcium salt of HA-*g*-PAA. (a) Residue of the injected insoluble salt seven days after injection. (b) The insoluble salt *ex vivo* seven days after injection. (c) A representative HE-stained sample of the insoluble salt a day after injection, 10×.

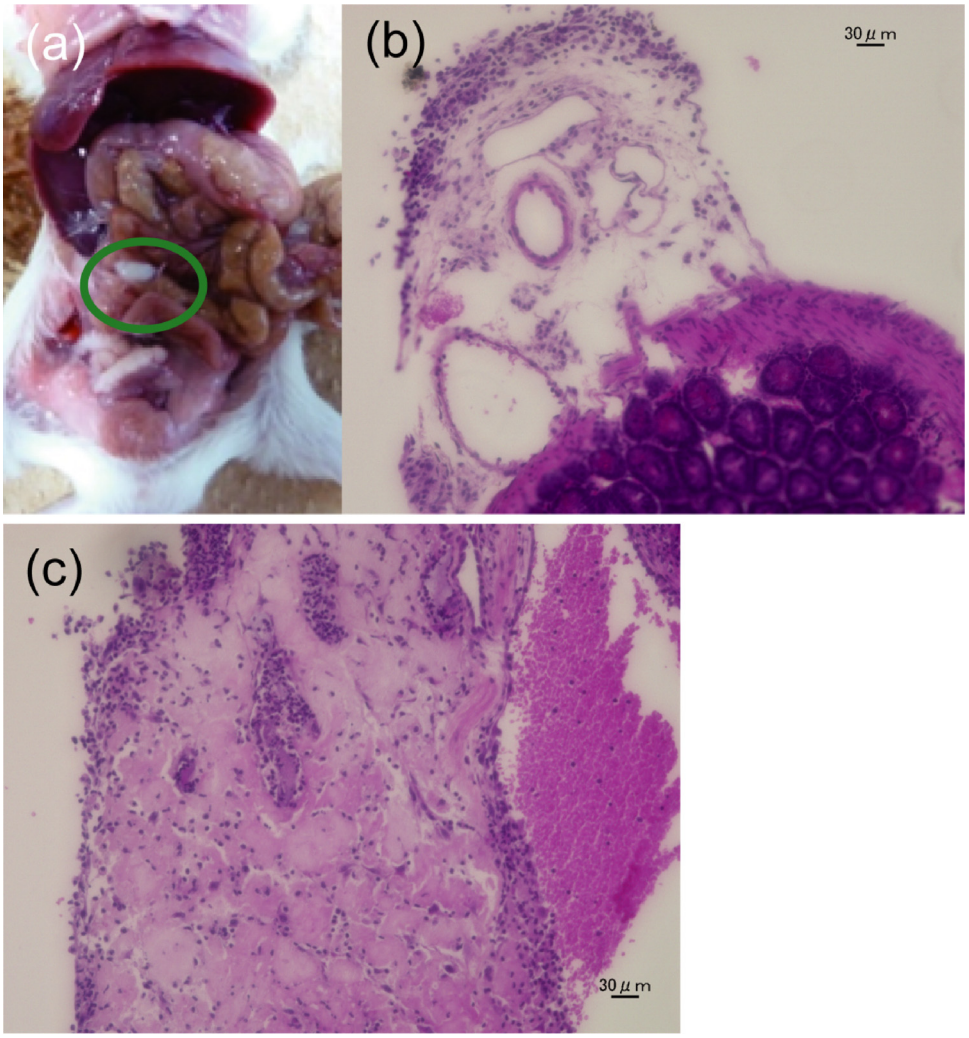

Fig. 8. Intraperitoneally administered insoluble calcium salt of HA-*g*-PAA seven days after injection ($N = 3$). Residues of the injected insoluble salt were found in two mice, while no residue was found in one mouse. (a) The adhered residue of the insoluble salt in the intestine. (b) HE-stained insoluble salt of (a), 20×. (c) HE staining of another residue that did not adhere to tissues, 20×.

the peritoneum. No decrease in the body weight was observed, and all of the mice showed a healthy condition. Transperitoneal pharmacokinetics was thoroughly investigated for peritoneal dialysis. There, polymers in which M_w was higher than 20 kDa were mainly removed by lymphatic processes, while polymers in which M_w was lower than 10 kDa were cleared by blood capillaries (Flessner, 2000). We speculate that HA-*g*-PAA was degraded into fragmented HA-*g*-PAA in the peritoneum mainly by carboxyesterases and lipases in peritoneal fluid based on the degradation kinetics *in vitro* shown in Fig. 4. Fragmented HA-*g*-PAA was probably cleared by the lymphatic system and/or blood vessels after passing through the peritoneal membrane by passive diffusion in the end.

These results and tendency did not change even when HA-*g*-PAA was administered as its insoluble salt by mixing with $CaCl_2$. Most of the insoluble salt was cleared from the peritoneum one week after injection. The HA-*g*-PAA insoluble salt would be gradually re-dissolved by exchanging Ca^{2+} ions to monovalent ions such as Na^+ and K^+ (which are abundant in peritoneal fluid) as shown in Fig. 5a, and then degraded and cleared like precursor HA-*g*-PAA polymers. On the other hand, the residence time of HA-*g*-PAA was prolonged by formation of the HA-*g*-PAA calcium salt, because we found a small amount of the injected HA-*g*-PAA calcium salt as shown in Fig. 8a. Considering that the residence time of native HA in the peritoneum is extremely short (half-life: ~3 h in rabbits and ~25.5 h in humans (Edelstam, Laurent, Lundkvist, Fraser, & Laurent, 1992; Johns & diZerega, 2000)), this prolonged residence time of insoluble calcium salt of HA-*g*-PAA, while maintaining biodegradability, would be advantageous. Inflammation around the injected HA-*g*-PAA calcium salt was mild in HE-stained pictures, as shown in Fig. 8b and c with the same level of dexamethasone-conjugated HA hydrogels (Ito et al., 2007a).

In this research, HA-based polymer was, for the first time to our knowledge, *in situ* cross-linked *in vivo* by calcium ions in a similar manner to the alginate/calcium ion system, which was quite effective and biocompatible in the peritoneum. Current commercially available antiperitoneal adhesion barriers are not strong enough to prevent severe adhesions (Shimizu et al., 2014). Also, HA-based *in situ* cross-linking hydrogels are expected to be useful for the treatment of peritoneal disseminations (Emoto et al., 2014). HA-*g*-PAA and its calcium salt have a high potential to be utilized for various applications in the peritoneum or other tissues in future.

4. Conclusion

We have succeeded in grafting PAA from HA for the first time via CRP in aqueous media. Grafting PAA from HA was an effective approach to controlling the degradation rate of native HA; HA-*g*-PAA showed slower degradation by HAse than native HA while exhibiting the scission of grafted PAA, short enough for kidney excretion, by hydrolysis and enzymatic degradation by lipase. In addition, HA-*g*-PAA formed an insoluble salt within a second by mixing with Ca^{2+} without utilizing chemically reactive moieties obtaining a solid material. Both HA-*g*-PAA and its calcium salt showed good biocompatibility, especially to mesothelial cells *in vitro*. Subcutaneous and intraperitoneal administration of HA-*g*-PAA or its calcium salt into mice was further performed *in vivo*. It was suggested that the residence time of HA-*g*-PAA was prolonged by formation of the insoluble calcium salt. In addition, no severe inflammation was observed around the materials. To the best of our knowledge, this is the first report on *in situ* cross-linking of HA-based polymers *in vivo* by calcium ions. HA-*g*-PAA would be a good candidate for drug delivery carriers in the peritoneum and for materials preventing peritoneal adhesion.

Acknowledgements

We deeply appreciate Kikkoman Biochemifa Co. for supplying hyaluronic acid, and Baxter for supplying the double-barrel syringe, and we also appreciate the aid of a Health Labor Sciences Research Grant from the Ministry of Health, Labor and Welfare of Japan (ID No. 10102883). S.O. appreciates the financial support of a Research Fellowship from the Japan Society for the Promotion of Science (JSPS).

References

Ahmed, T. A. E., Dare, E. V., & Hincke, M. (2008). Fibrin: A versatile scaffold for tissue engineering applications. *Tissue Engineering, B—Reviews*, *14*(2), 199–215.

Ashford, E. J., Naldi, V., O'Dell, R., Billingham, N. C., & Armes, S. P. (1999). First example of the atom transfer radical polymerisation of an acidic monomer: Direct synthesis of methacrylic acid copolymers in aqueous media. *Chemical Communications*, *14*, 1285–1286.

Bitter, T., & Muir, H. M. (1962). A modified uronic acid carbazole reaction. *Analytical Biochemistry*, *4*, 330–334.

Brenner, B. M., Hostetter, T. H., & Humes, H. D. (1978). Glomerular permselectivity: Barrier function based on discrimination of molecular size and charge. *American Journal of Physiology*, *234*(6), F455–F460.

Bulpitt, P., & Aeschlimann, D. (1999). New strategy for chemical modification of hyaluronic acid: Preparation of functionalized derivatives and their use in the formation of novel biocompatible hydrogels. *Journal of Biomedical Materials Research*, *47*(2), 152–169.

Chang, N. S., & Boackle, R. J. (1985). Hyaluronic-acid complement interactions. 2. Role of divalent-cations and gelatin. *Molecular Immunology*, *22*(8), 843–848.

Chen, Y., Liu, Y. F., & Tan, H. M. (2010). Hydroxyethyl chitosan-g-poly(acrylic acid-*co*-sodium acrylate) superabsorbent polymers. *Journal of Applied Polymer Science*, *117*(4), 2233–2240.

Coullerez, G., Carlmark, A., Malmstrom, E., & Jonsson, M. (2004). Understanding copper-based atom-transfer radical polymerization in aqueous media. *Journal of Physical Chemistry A*, *108*(35), 7129–7131.

Delmage, J. M., Powars, D. R., Jaynes, P. K., & Allerton, S. E. (1986). The selecive suppression of immunogenicity by hyaluronic acid. *Annals of Clinical and Laboratory Science*, *16*(4), 303–310.

Edelstam, G. B., Laurent, U. G., Lundkvist, Ö., Fraser, J. R., & Laurent, T. (1992). Concentration and turnover of intraperitoneal hyaluronan during inflammation. *Inflammation*, *16*(5), 459–469.

Emoto, S., Yamaguchi, H., Kamei, T., Ishigami, H., Suhara, T., Suzuki, Y., et al. (2014). Intraperitoneal administration of cisplatin via an in situ cross-linkable hyaluronic acid-based hydrogel for peritoneal dissemination of gastric cancer. *Surgery Today*, *44*(5), 919–926.

Flessner, M. F. (2000). Transperitoneal pharmacokinetics. In G. S. Dizerega (Ed.), *Peritoneal surgery* (pp. 421–440). New York, NY: Springer-Verlag New York Inc.

Gabriel, D. A., & Carr, M. E. (1989). Calcium destabilizes and causes conformational changes in hyaluronic acid. *American Journal of the Medical Sciences*, *298*(1), 8–14.

Gilli, R., Kacurakova, M., Mathlouthi, M., Navarini, L., & Paoletti, S. (1994). FTIR studies of sodium hyaluronate and its oligomers in the amorphous solid phase and in aqueous solution. *Carbohydrate Research*, *263*(2), 315–326.

Harada, H., & Takahashi, M. (2007). CD44-dependent intracellular and extracellular catabolism of hyaluronic acid by hyaluronidase-1 and-2. *Journal of Biological Chemistry*, *282*(8), 5597–5607.

Hardingham, T. (2004). Solution properties of hyaluronan. In H. G. Garg, & C. A. Hales (Eds.), *Chemistry and biology of hyaluronan* (pp. 1–20). Oxford: Elsevier Ltd.

Hrabarova, E., Rychly, J., Sasinkova, V., Valachova, K., Janigova, I., Csomorova, K., et al. (2012). Structural characterisation of thiol-modified hyaluronans. *Cellulose*, *19*(6), 2093–2104.

Huber, K. (1993). Calcium-induced shrinking of polyacrylate chains in aqueous-solution. *Journal of Physical Chemistry*, *97*(38), 9825–9830.

Ito, T., Fraser, I. P., Yeo, Y., Highley, C. B., Bellas, E., & Kohane, D. S. (2007). Anti-inflammatory function of an in situ cross-linkable conjugate hydrogel of hyaluronic acid and dexamethasone. *Biomaterials*, *28*(10), 1778–1786.

Ito, T., Yeo, Y., Highley, C. B., Bellas, E., Benitez, C. A., & Kohane, D. S. (2007). The prevention of peritoneal adhesions by in situ cross-linking hydrogels of hyaluronic acid and cellulose derivatives. *Biomaterials*, *28*(6), 975–983.

Jin, R., Teixeira, L. S. M., Krouwels, A., Dijkstra, P. J., van Blitterswijk, C. A., Karperien, M., et al. (2010). Synthesis and characterization of hyaluronic acid–poly(ethylene glycol) hydrogels via Michael addition: An injectable biomaterial for cartilage repair. *Acta Biomaterialia*, *6*(6), 1968–1977.

Johns, D. B., & diZerega, G. S. (2000). Development and clinical evaluation of intergel adhesion prevention solution for the reduction of adhesions following peritoneal cavity surgery. In G. S. Dizerega (Ed.), *Peritoneal surgery* (pp. 351–366). New York, NY: Springer-Verlag New York Inc.

Kacurakova, M., Capek, P., Sasinkova, V., Wellner, N., & Ebringerova, A. (2000). FT-IR study of plant cell wall model compounds: Pectic polysaccharides and hemicelluloses. *Carbohydrate Polymers*, *43*(2), 195–203.

Kaewprapan, K., Inprakhon, P., Marie, E., & Durand, A. (2012). Enzymatically degradable nanoparticles of dextran esters as potential drug delivery systems. *Carbohydrate Polymers*, *88*(3), 875–881.

Konkolewicz, D., Krys, P., Góis, J. R., Mendonça, P. V., Zhong, M., Wang, Y., et al. (2014). Aqueous RDRP in the presence of Cu0: The exceptional activity of CuI confirms the SARA ATRP mechanism. *Macromolecules*, *47*(2), 560–570.

La Gatta, A., De Rosa, M., Marzaioli, I., Busico, T., & Schiraldi, C. (2010). A complete hyaluronan hydrodynamic characterization using a size exclusion chromatography–triple detector array system during in vitro enzymatic degradation. *Anal. Biochem.*, *404*(1), 21–29.

La Gatta, A., Schiraldi, C., Papa, A., D'Agostino, A., Cammarota, M., De Rosa, A., et al. (2013). Hyaluronan scaffolds via diglycidyl ether crosslinking: Toward improvements in composition and performance. *Carbohydrate Polymers*, *96*(2), 536–544.

Laurent, T. C., & Fraser, J. R. E. (1992). Hyaluronan. *Faseb Journal*, *6*(7), 2397–2404.

Lepperdinger, G., Fehrer, C., & Reitinger, S. (2004). Biodegradation of hyaluronan. In H. G. Garg, & C. A. Hales (Eds.), *Chemistry and biology of hyaluronan* (pp. 71–82). Oxford: Elsevier Ltd.

Matyjaszewski, K., & Xia, J. H. (2001). Atom transfer radical polymerization. *Chemical Reviews*, *101*(9), 2921–2990.

Mazumder, M. A. J., Fitzpatrick, S. D., Muirhead, B., & Sheardown, H. (2012). Cell-adhesive thermogelling PNIPAAm/hyaluronic acid cell delivery hydrogels for potential application as minimally invasive retinal therapeutics. *Journal of Biomedical Materials Research, A*, *100A*(7), 1877–1887.

Mishra, S., Rani, G. U., & Sen, G. (2012). Microwave initiated synthesis and application of polyacrylic acid grafted carboxymethyl cellulose. *Carbohydrate Polymers*, *87*(3), 2255–2262.

Mortisen, D., Peroglio, M., Alini, M., & Eglin, D. (2010). Tailoring thermoreversible hyaluronan hydrogels by click chemistry and RAFT polymerization for cell and drug therapy. *Biomacromolecules*, *11*(5), 1261–1272.

Ostmark, E., Harrisson, S., Wooley, K. L., & Malmstrom, E. E. (2007). Comb polymers prepared by ATRP from hydroxypropyl cellulose. *Biomacromolecules*, *8*(4), 1138–1148.

Pal, S., & Pal, A. (2012). Synthesis and characterizing a novel polymeric flocculant based on amylopectin-graft-polyacrylamide-graft-polyacrylic acid (AP-g-PAM)-g-PAA. *Polymer Bulletin*, *69*(5), 545–560.

Percec, V., Guliashvili, T., Ladislaw, J. S., Wistrand, A., Stjerndahl, A., Sienkowska, M. J., et al. (2006). Ultrafast synthesis of ultrahigh molar mass polymers by metal-catalyzed living radical polymerization of acrylates, methacrylates, and vinyl chloride mediated by SET at 25 degrees C. *Journal of the American Chemical Society*, *128*(43), 14156–14165.

Pitarresi, G., Fiorica, C., Licciardi, M., Palumbo, F. S., & Giammona, G. (2013). New hyaluronic acid based brush copolymers by atom transfer radical polymerization. *Carbohydrate Polymers*, *92*(2), 1054–1063.

Pourjavadi, A., Harzandi, A. M., & Hosseinzadeh, H. (2004). Modified carrageenan 3. Synthesis of a novel polysaccharide-based superabsorbent hydrogel via graft copolymerization of acrylic acid onto kappa-carrageenan in air. *European Polymer Journal*, *40*(7), 1363–1370.

Rosen, B. M., & Percec, V. (2009). Single-electron transfer and single-electron transfer degenerative chain transfer living radical polymerization. *Chemical Reviews*, *109*(11), 5069–5119.

Roy, D., Semsarilar, M., Guthrie, J. T., & Perrier, S. (2009). Cellulose modification by polymer grafting: A review. *Chemical Society Reviews*, *38*(7), 2046–2064.

Schanté, C., Zuber, G., Herlin, C., & Vandamme, T. F. (2011). Synthesis of *N*-alanyl-hyaluronamide with high degree of substitution for enhanced resistance to hyaluronidase-mediated digestion. *Carbohydrate Polymers*, *86*(2), 747–752.

Schanté, C. E., Zuber, G., Herlin, C., & Vandamme, T. F. (2012). Improvement of hyaluronic acid enzymatic stability by the grafting of amino-acids. *Carbohydrate Polymers*, *87*(3), 2211–2216.

Schweins, R., & Huber, K. (2001). Collapse of sodium polyacrylate chains in calcium salt solutions. *European Physical Journal E*, *5*(1), 117–126.

Shimizu, A., Suhara, T., Ito, T., Omichi, K., Naruse, K., Hasegawa, K., et al. (2014). A new hepatectomy-induced postoperative adhesion model in rats, and evaluation of the efficacy of anti-adhesion materials. *Surgery Today*, *44*(2), 314–323.

Shu, X. Z., Liu, Y. C., Luo, Y., Roberts, M. C., & Prestwich, G. D. (2002). Disulfide cross-linked hyaluronan hydrogels. *Biomacromolecules*, *3*(6), 1304–1311.

Strauss, E. J., Hart, J. A., Miller, M. D., Altman, R. D., & Rosen, J. E. (2009). Hyaluronic acid viscosupplementation and osteoarthritis: Current uses and future directions. *American Journal of Sports Medicine*, *37*(8), 1636–1644.

Su, W.-Y., Chen, Y.-C., & Lin, F.-H. (2010). Injectable oxidized hyaluronic acid/adipic acid dihydrazide hydrogel for nucleus pulposus regeneration. *Acta Biomaterialia*, *6*(8), 3044–3055.

Takahashi, A., Suzuki, Y., Suhara, T., Omichi, K., Shimizu, A., Hasegawa, K., et al. (2013). In situ cross-linkable hydrogel of hyaluronan produced via copper-free click chemistry. *Biomacromolecules*, *14*(10), 3581–3588.

Tan, H. P., Ramirez, C. M., Miljkovic, N., Li, H., Rubin, J. P., & Marra, K. G. (2009). Thermosensitive injectable hyaluronic acid hydrogel for adipose tissue engineering. *Biomaterials*, *30*(36), 6844–6853.

Tanaka, S., Oka, S., Kaneko, I., Hirata, M., Mouri, R., Kanao, H., et al. (2007). Endoscopic submucosal dissection for colorectal neoplasia: Possibility of standardization. *Gastrointestinal Endoscopy*, *66*(1), 100–107.

Thermes, F., Grove, J., Rozier, A., Plazonnet, B., Constancis, A., Bunel, C., et al. (1992). Mucoadhesion of copolymers and mixtures containing polyacrylic acid. *Pharmaceutical Research*, *9*(12), 1563–1567.

Yamaoka, T., Tabata, Y., & Ikada, Y. (1994). Distribution and tissue uptake of poly(ethylene glycol) with different molecular-weights after intravenous administration to mice. *Journal of Pharmaceutical Sciences*, *83*(4), 601–606.

Yeo, Y., Burdick, J. A., Highley, C. B., Marini, R., Langer, R., & Kohane, D. S. (2006). Peritoneal application of chitosan and UV-cross-linkable chitosan. *Journal of Biomedical Materials Research, A*, *78A*(4), 668–675.

Yeo, Y., Highley, C. B., Bellas, E., Ito, T., Marini, R., Langer, R., et al. (2006). In situ cross-linkable hyaluronic acid hydrogels prevent post-operative abdominal adhesions in a rabbit model. *Biomaterials*, *27*(27), 4698–4705.

Yokoi, N., Komuro, A., Nishida, K., & Kinoshita, S. (1997). Effectiveness of hyaluronan on corneal epithelial barrier function in dry eye. *British Journal of Ophthalmology*, *81*(7), 533–536.

Zheng Shu, X., Liu, Y., Palumbo, F. S., Luo, Y., & Prestwich, G. D. (2004). In situ crosslinkable hyaluronan hydrogels for tissue engineering. *Biomaterials*, *25*(7–8), 1339–1348.

Zhong, S. P., Campoccia, D., Doherty, P. J., Williams, R. L., Benedetti, L., & Williams, D. F. (1994). Biodegradation of hyaluronic acid derivatives by hyaluronidase. *Biomaterials*, *15*(5), 359–365.